Towards an Archaeological Index: Identification of the Spectral Regions of Stress Vegetation due to Buried Archaeological Remains

Athos Agapiou[1], Diofantos G. Hadjimitsis[1], Andreas Georgopoulos[2], Apostolos Sarris[3] and Dimitrios D. Alexakis[1]

[1] [1]Department of Civil Engineering and Geomatics, Faculty of Engineering and Technology, Cyprus University of Technology, 3603, Limassol, Cyprus
{athos.agapiou, d.hadjimitsis, k.themistocleous, dimitrios.alexakis}@cut.ac.cy
[2]Laboratory of Photogrammetry, School of Rural & Surveying Engineering, NTUA, Greece
drag@central.ntua.gr
[3]Laboratory of Geophysical - Satellite Remote Sensing and Archaeo-environment, Institute for Mediterranean Studies, Foundation for Research & Technology, Hellas (F.O.R.T.H.), 74100, Rethymno, Crete, Greece
asaris@ret.forthnet.gr

Abstract. This paper aims to introduce the spectral characteristics of a new Archaeological Index. This index will be able to enhanced crop marks, recorded in multispectral / hyperspectral remote sensing images, which are related to buried archaeological remains. Spectral signatures were acquired from two agricultural areas of Cyprus (Alampra and Acheleia), specifically constructed in order to simulate buried archaeological remains. A complete phenological cycle of barley and wheat crops was observed using ground spectroradiometer with spectral range from 350 – 1050 nm (visible – near infrared spectrum). Correlation regression and different separability indices were then applied in the whole dataset in order to isolate the narrow band spectrum where stress vegetation characteristics are maximized. The results were found similar for both sites –regardless crop type- and the spectral sensitivity was detected at the red edge and near infrared spectrum (≈ 700 and ≈ 800 nm).

Keywords: archaeological index; crop marks; experimental remote sensing archaeology; buried archaeological remains; separability index

1 Introduction

Detection of buried archaeological remains is usually performed based on different vegetation indices such as the Normalized Difference Vegetation Index (NDVI) and Simple Ratio (SR). These indices are used to enhance crop marks which are related to archaeological features. Indeed the results are very promising and indicate that vegetation indices can be applied in multispectral or hyperspectral dataset for the archaeological research [1-5].

Nevertheless the use of a specific index for monitoring such crop marks has never been discussed or performed in the past. This is due to the fact that crop marks constitute a complicated phenomenon and difficult to be modeled, since several parameters should be taken into consideration. Such parameters are for example the characteristics of the buried features, the burial depth of them, soil characteristics, climatic and environmental parameters, cultivation techniques, etc [6].

This paper aims to evaluate the above hypothesis. For the aims of the study several ground truth measurements over vegetation with and with-out buried archaeological remains were acquired for a whole phenological cycle from two different cases studies with different cultivation techniques and crop types. This is the first time that such evaluation is performed for the context of archaeological research.

2 Experimental Remote Sensing

Experimental Remote Sensing is a new scientific field [6] where remote sensing techniques are used for the detection of a-priori known archaeological targets. In contrary to Remote Sensing Archaeology where vegetation anomalies can be only confirmed after an archaeological excavation, Experimental Remote Sensing is focused to understand the characteristics of the anomaly formation based on known buried features. For the aims of the study two test fields were constructed at different agricultural areas of Cyprus. The first case study is located near the Alampra village, central Cyprus, while the second case study is placed in the Acheleia area, southwest of Cyprus.

Eight "control" sites of size 5 x 5 sq.m have been prepared in the Alampra test field. Each of this sites aimed to simulate different archaeological environments. The first two squares were used to simulate "tombs" at a depth of 25 cm (Sites 1-2); in the next two sampling squares (Sites 3-4) local stones have been buried at a depth of 25 cm while in another two squares similar stones were buried at a depth of 50 cm (Sites 5-6). Moreover, the last two squares (Sites 7-8) were left untouched. Local stones were collected from the area of Alampra and used in the control field. All squares are placed in the same parcel in order to minimize any differences in environmental, meteorological or soil conditions. All sites have been cultivated with barley crops according to the traditional methods of the area (Fig. 1).

A similar approach was performed to Acheleia area. One "control" site was constructed where local stones were placed at a depth of 25cm below ground surface. The area was then cultivated with wheat crop (Fig. 2).

Fig. 1. Photos during the construction of the test field in Alampra area. Local stones are placed at a depth of 25 cm below ground surface and then barley crop was cultivated.

Fig. 2. Photos during the construction of the test field in Acheleia area. Local stones are placed at a depth of 25 cm below ground surface and then wheat crop was cultivated.

3 Ground Measurements

Ground spectroradiometric measurements were acquired during the complete phenological cycle of the crop during the period of 2011 -2012. In total, more than 16 in-situ campaigns were performed for each one of the case study areas (Alampra and Acheleia). In each campaign the GER 1500 spectroradiometer was used along with a reference calibrated panel. The specific instrument has the ability to record electromagnetic radiation from 350 until 1050 nm, with a 1.5 nm interval measurement. Reflectance values were measured using Equation 1:

$$\text{Reflectance} = (\text{Target Radiance} / \text{Panel Radiance}) \times \text{Calibration of the panel} \quad (1)$$

More than 1900 ground measurements were acquired in the Alampra test field and 700 spectroradiometric measurements in the Acheleia area. Mean reflectance values from each campaign were used in order to create a spectral library of each crop, barley and wheat, for the whole phenological stages of the plant. A typical example of spectral signature for barley crop at the early stage of turgor is shown in Fig. 3.

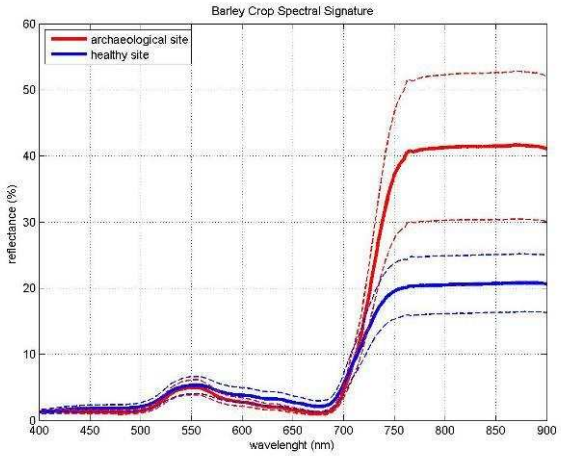

Fig. 3. Typical spectral signature for barley crop, at the early stage of turgor, over simulated archaeological environment (red line) and healthy vegetation (blue line).

4 Post-processing of Ground Measurements

The analysis of the data derived from in situ campaigns has been performed into two different steps: (a) correlation analysis and (b) separability analysis. The results of the post-processing are shown below.

4.1 Correlation Analysis

A simple way to examine all the data from the different ground spectroradiometric campaigns is to correlate the spectral signature value of a specific wavelength to all the rest wavelengths. The Pearson correlation coefficient, also known as R, is used to measure the strength of the linear relationship between two variables.

As it is found from Figs. 4 and 5 a low correlation is observed between the range 750-900nm against 530-570nm. Moreover a minimum correlation is also recorded in the red edge spectrum (around 700nm).

The first low correlation observation refers to the spectral characteristics of vegetation close to the near infrared and green wavelengths. A typical spectral signature of vegetation is expected to have very low reflectance in the blue and red wavelength regions, slightly higher in the green area and high in the near infrared. This result highlights the fact that even though the plant seems to be growing under non stressed conditions (green wavelength, visible to the human eye), this may be quite different in the near infrared reflectance (since green and near infrared spectrum are "unrelated" to each other). So if the normal process of the plant is disturbed (i.e. period of stress), this might not be early detected from just visual observations of the

plant. Indeed several researches agree that when a plant is growing under stress conditions, this is expressed either with visible or non visible symptoms.

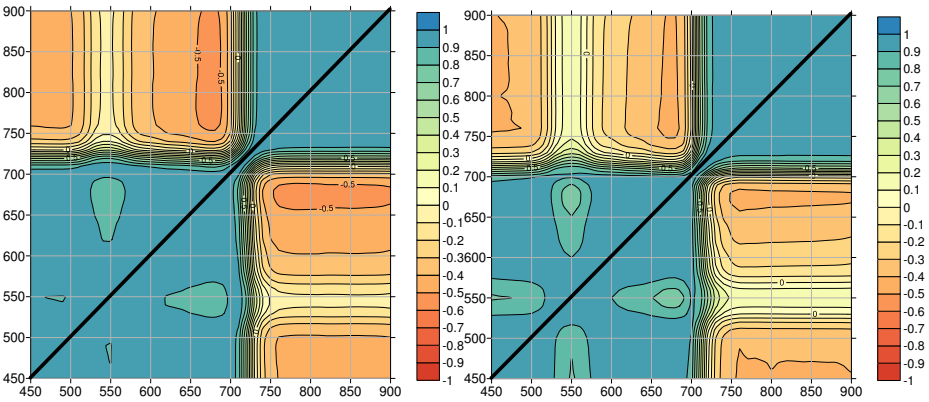

Fig. 4. Correlation analysis of the narrow band wavelength from 450 -900 nm (visible- near infrared spectrum) versus reflectance values from Alampra test field -barley crops- (top) and Acheleia case study -wheat crops- (bottom).

4.2 Separability Indices

In an effort to identify spectral regions which are capable to distinguish the spectral diversity of vegetation due to archaeological remains, several indicators (algorithms) were used. These algorithms are often called Separability Indices, since they are used in order to examine the separability of two variables. The purpose of these indicators is to identify whether a group of observations X is separable from another group of observations Y. For the aims of the study three mains Separability Indices were performed for the two case study areas in Alampra and Acheleia: (a) Euclidean distance, (b) Mahalanobis distance and (c) cosine similarity.

The above three Separability Indices are widely used in classification techniques for satellite images. The Euclidean distance is used mainly in classifications where the minimum distance algorithm is applied, the Mahalanobis distance in the classification using the maximum likelihood method and parallelepiped classification. Finally the cosine similarity index is exploited to Spectral Angle Mapper (SAM) classification techniques.

Euclidean distance. This method simply calculates the Euclidean distance between a pair of observations. The mathematical equation of Euclidean distance is presented in Equation 2, while the results for both case studies are tabulated in Table 1.

$$d = (p_x - q_x) \quad (2)$$

Where:
d: Euclidean distance
p_x: radiation in a specific wavelength for the first group of observations (healthy vegetation)
q_x: radiation in a specific wavelength for the second group of observations (stress vegetation due to archaeological remains).

Table 1. Separability results for Alampra (top) and Acheleia (bottom) case study using the Euclidean distance algorithm. In grey the highest separability values recorded.

Wavelength (nm)	450	500	550	600	650	700	750	800	850	900
450	0.0									
500	1.5	0.0								
550	6.0	4.6	0.0							
600	6.0	4.5	0.1	0.0						
650	5.8	4.4	0.2	0.1	0.0					
700	9.4	8.0	3.4	3.5	3.6	0.0				
750	27.9	26.5	22.0	22.1	22.2	18.7	0.0			
800	31.0	29.5	25.0	25.1	25.2	21.7	3.1	0.0		
850	31.9	30.4	26.0	26.0	26.1	22.7	4.0	0.9	0.0	
900	32.1	30.7	26.2	26.3	26.4	22.9	4.2	1.2	0.2	0.0

Wavelength (nm)	450	500	550	600	650	700	750	800	850	900
450	0.0									
500	1.5	0.0								
550	5.2	3.7	0.0							
600	7.7	6.2	2.5	0.0						
650	8.7	7.2	3.5	1.0	0.0					
700	11.5	10.1	6.3	3.8	2.9	0.0				
750	23.3	21.8	18.0	15.6	14.6	11.7	0.0			
800	26.0	24.5	20.8	18.3	17.3	14.5	2.7	0.0		
850	27.0	25.5	21.8	19.3	18.4	15.5	3.8	1.0	0.0	
900	27.6	26.2	22.4	20.0	19.0	16.1	4.4	1.6	0.6	0.0

Mahalanobis distance. This method is similar to the Euclidean distance but it also exploits the covariance matrix of the measurements. The mathematical equation for Mahalonobis distance is given in Equation 3. Separability results for Alampra and Acheleia case study is shown in Table 2. Grey values indicate the highest separability recorded from all dataset.

$$d_{mahalanobis} = (p_x - q_x)\, C^{-1} \quad (3)$$

Where:
$d_{mahalanobis}$: Mahalanobis distance
C: Covariance matrix
p_x: radiation in a specific wavelength for the first group of observations (healthy vegetation)
q_x: radiation in a specific wavelength for the second group of observations (stress vegetation due to archaeological remains)

Table 2. Separability results for Alampra (top) and Acheleia (bottom) case study using the Mahalonobis distance algorithm. In grey the highest separability values recorded.

Wavelength (nm)	450	500	550	600	650	700	750	800	850	900
450	0.0									
500	0.5	0.0								
550	1.9	1.4	0.0							
600	2.0	1.6	0.1	0.0						
650	1.9	1.4	0.0	0.1	0.0					
700	3.2	2.7	1.3	1.1	1.3	0.0				
750	2.9	2.6	1.7	1.7	1.7	1.8	0.0			
800	2.6	2.4	2.1	2.2	2.1	2.7	1.0	0.0		
850	2.7	2.5	2.2	2.2	2.2	2.7	1.0	0.1	0.0	
900	2.8	2.5	2.1	2.2	2.1	2.6	0.8	0.3	0.2	0.0

Wavelength (nm)	450	500	550	600	650	700	750	800	850	900
450	0.0									
500	0.5	0.0								
550	1.4	0.9	0.0							
600	2.6	2.1	1.2	0.0						
650	3.0	2.5	1.6	0.4	0.0					
700	3.6	3.2	2.2	1.0	0.6	0.0				

750	2.7	2.4	1.8	1.9	2.1	2.3	0.0			
800	2.8	2.5	2.1	2.3	2.5	2.7	0.4	0.0		
850	2.9	2.6	2.2	2.3	2.5	2.7	0.4	0.1	0.0	
900	3.1	2.8	2.2	2.2	2.4	2.6	0.4	0.4	0.2	0.0

Cosine similarity. The cosine similarity refers to the similarity between two vectors by calculating the cosine of the angle formed by these vectors. The cosine similarity is given by Equation 4. The final results from the Cosine similarity index are shown in Table 3. Grey values indicate the highest seperablity recorded from all dataset.

$$d_{\text{cosine simillarity}} = \cos(\varphi) = 1 - (p_x . q_x^T) / ((p_x . p_x^T)(q_x . q_x^T))^{0.5} \quad (4)$$

Where:
p_x: radiation in a specific wavelength for the first group of observations (healthy vegetation)
q_x: radiation in a specific wavelength for the second group of observations (stress vegetation due to archaeological remains)

Table 3. Separability results for Alampra (top) and Acheleia (bottom) case study using the Cosine similarity algorithm. In grey the highest separability values recorded.

Wavelength (nm)	450	500	550	600	650	700	750	800	850	900
450	.0000									
500	.0000	.0000								
550	.0001	.0000	.0000							
600	.0001	.0000	.0000	.0000						
650	.0002	.0001	.0000	.0000	.0000					
700	.0000	.0000	.0001	.0001	.0002	.0000				
750	.0119	.0108	.0101	.0103	.0093	.0123	.0000			
800	.0162	.0149	.0141	.0143	.0131	.0166	.0003	.0000		
850	.0141	.0129	.0121	.0123	.0112	.0145	.0001	.0001	.0000	
900	.0162	.0149	.0141	.0143	.0131	.0166	.0003	.0000	.0001	.0000

Wavelength (nm)	450	500	550	600	650	700	750	800	850	900
450	.00									
500	.0000	.00								

550	.0000	.0000	.00							
600	.0000	.0000	.0000	.00						
650	.0000	.0000	.0000	.0000	.00					
700	.0000	.0000	.0000	.0000	.0000	.00				
750	.0005	.0005	.0004	.0007	.0008	.0006	.00			
800	.0006	.0006	.0006	.0008	.0009	.0008	.0000	.00		
850	.0006	.0007	.0006	.0008	.0009	.0008	.0000	.0000	.00	
900	.0006	.0006	.0005	.0008	.0009	.0007	.0000	.0000	.0000	.00

Based on the previous results it seems that spectral differences of vegetation are more distinct, regardless the seperablity index or crop type, at the near infrared and blue wavelengths. Also high seperablity values are recorded at the near infrared and red wavelength. Although the latter is expected since these features are exploited by various vegetation indices, the first case requires further investigation since atmospheric effect can not be ignored in this part of the spectrum. Blue channel is used in specialized indices (e.g. ARVI, SARVI, ARI) for removal of atmospheric effects of the image. Scattering is a phenomenon observed in short wavelengths due to highest Rayleigh scattering. Therefore non atmospheric corrected images are expected to be particularly noisy in hazy days.

5 Conclusions

This paper aimed to identify the spectral characteristics of an archaeological index using a large database of spectral signatures taken over two different cases studies. The measurements were taken for the whole phenological cycle of barley and wheat crops. Experimental Remote Sensing benefits are also highlighted.

The development of a special Archaeological Index for detection of crop marks is a difficult task due to the numerous parameters that should be taken into consideration. Based on the findings of the previous analysis it is shown that multispectral sensors which are sensitive to near infrared wavelengths are able to record the different variations occurred at vegetation due to the existence of buried archaeological remains. Significant spectral differences, with the exception of the blue wavelength, seem to exist in the region of around 800nm to 700nm (near infrared and red edge).

Therefore an archaeological index which will be able to record variations of vegetation due to archaeological remains should be focus on the spectral characteristics close to 800nm to 700nm in atmospherically corrected images. This indicator should follow the following function:

$$\text{A.I.} = f(p \approx 800, p \approx 700) \quad (5)$$

Where
A.I.: Archaeological index
$p \approx 800$: reflectance at around 800 nm
$p \approx 700$: reflectance at around 700 nm

Based on the results of this study any potential user is able to distinguish which of the available vegetation indices that exist in the literature may be used to detect subsurface features. It should be mentioned that this conclusion is in complete agreement with previous results performed by the authors [7] regarding the spectral sensitivity of different satellite sensors. In that study the IKONOS satellite was found to be the most sensitive to the vegetation variations. This is related to the spectral sensitivity of the sensor.

Acknowledgments. These results are part of the PhD dissertation of Mr. Athos Agapiou. The authors would like to express their appreciation to the Alexander Onassis Foundation for funding the PhD study. Also thanks are given to the Remote Sensing Laboratory of the Department of Civil Engineering & Geomatics at the Cyprus University of Technology for the support (http://www.cut.ac.cy/).

References

1. Lasaponara, R., Masini, N.: Satellite remote sensing in archaeology: past, present and future perspectives. JARS, 38(9), 1995-2002 (2011).
2. Agapiou, A., Hadjimitsis, D. G.: Vegetation indices and field spectro-radiometric measurements for validation of buried architectural remains: verification under area surveyed with geophysical campaigns. Journal of Applied Remote Sensing, 5, 053554-1 (2011)
3. Alexakis, D., Sarris, A., Astaras, T., Albanakis, K. : Integrated GIS, remote sensing and geomorphologic approaches for the reconstruction of the landscape habitation of Thessaly during the Neolithic period. JARS,, 38, 89-100 (2011).
4. Traviglia, A.: Integration of MIVIS Hyperspectral remotely sensed data and Geographical Information Systems to study ancient landscape: the Aquileia case study. An International Journal of Landscape Archaeology, 2, 139-170 (2005).
5. Rowlands, A. Sarris, A.: Detection of Exposed and Subsurface Archaeological Remains using Multi-Sensor Remote Sensing. JARS, 34, 795-803 (2007).
6. Agapiou, A., Hadjimitsis, D. G., Sarris, A., Georgopoulos, A.: A New Method for the Detection Validation of Architectural Remains Using Field Spectroscopy: Experimental Remote Sensing Archaeology. In: Proceedings XVI Congress of the UISPP (International Union for Prehistoric and Protohistoric Sciences), 4 - 10 September, Florianopolil, Brazil (in press).
7. Agapiou, A., Alexakis, D., Hadjimitsis, D. G.: Evaluation of spectral sensitivity of ALOS, ASTER, IKONOS, LANDSAT and SPOT satellite sensors intended for the detection of archaeological crop marks, Digital Earth, DOI:10.1080/17538947.2012.674159. (2012).